INTERNATIONAL SYMPOSIUM
ON FLOW VISUALIZATION
Bochum, 9.-12. Sept. 1980

Preprints of contributed papers

IN-LINE HOLOGRAPHY FOR FLOW AND CAVITATION VISUALIZATION ON HYDROFOILS AND FOR NUCLEI MEASUREMENTS

R.L. van Renesse* and J.H.J. van der Meulen**

* Institute of Applied Physics TNO-TH, Delft, The Netherlands

** Netherlands Ship Model Basin, Wageningen, The Netherlands

The boundary layer flow about two hydrofoils and the appearance of cavitation are investigated by means of in-line holography. Practical details on the hologram resolution and data collection time for nuclei size analysis are given. It is shown that the appearance of cavitation on the hydrofoils is strongly influenced by viscous effects.

1. INTRODUCTION

In-line holography has been used before to visualize the boundary layer flow in water on axisymmetric bodies [1, 2]. These and other studies have shown that cavitation on axisymmetric bodies is closely related to viscous effects. In order to investigate possible relationships between types of cavitation occurring on hydrofoils and the complex boundary layer flow behaviour, further studies were made making use of in-line holography. The experiments were made in a high speed water tunnel, provided with a 40 mm x 80 mm rectangular test section. Two hydrofoils with a 70 mm chord were tested: a NACA 16-012 profile and a NACA 4412 profile. Boundary layer flow visualization was effected by injecting a 5 percent sodium chloride solution from a hole (dia. 0.21 mm) located at the leading edge of the hydrofoil. The present paper comprises details on the holographic procedure and displays some typical boundary layer flow and cavitation phenomena.

2. HOLOGRAPHIC EXPERIMENTAL PROCEDURE

Fig. 1 shows a diagram of the in-line holographic set-up applied. A ruby-laser (λ=694nm) with a 30 mJ single mode pulse duration of 30ns was used as a light source, serving a plane parallel beam of 80 mm diameter with the aid of a telescopic system. Fig. 2 gives a schematic view of the exposure and subsequent reconstruction of the holographed test volume. The light waves scattered by an object interfere with the uninterrupted background waves thus causing a fringe pattern that is recorded on the hologram. Typical fringe patterns are shown in Fig. 3. Agfa-Gevaert 8E75 Holotest plates were used as a recording medium. In the reconstruction set-up a 2mW HeNe-laser (λ=633nm) serves as a light source. The recorded fringe patterns diffract the incident light into positive and negative diffraction orders thus creating a real as well as a virtual image of the original object. In the case of applying plane parallel beams in both the recording and the reconstruction step, the magnification of the reconstructed image equals unity irrespective of the difference in wavelength between the recording and the reconstructing beam. With the aid of a microscope the real image of the test volume may now be analyzed, yielding absolute data for particle size- and particle density distributions as well as further data relevant for flow and cavitation analysis. For a detailed analysis of in-line holography reference is made to the relevant literature [3].

Although the in-line holographic technique is a unique means for analyzing the particle content of relatively large volumes (typically tens of cubic centimeters) it has been recognized that the reading out of the holograms is rather laborious. Bexon et al. [4] state that at best 400 particles can be sized in 7 hours and that there is evidence to suggest that the operator becomes erratic as time passes. Gates et al. [5] mention that typically 200 particles per hologram are analyzed and that this requires about one man-day. Earlier work [6] has shown that for low to moderate concentrations the read out time tends to be inversely proportional to concentration (Fig. 4). The average concentration measured from a total of 30 holograms (3 bubbles per cubic centimeter) gave rise to an average read out time of 2 minutes per bubble. This figure coincides with that of Gates et al. The optimum figure

given by Bexon et al. is only improved at relatively high concentrations (>10 bubbles per cubic centimeter). However, if concentrations become too large and the laserbeam has to penetrate through a considerable depth of particle cloud, optical noise will spoil the quality of the reconstruction. The data of Fig. 4 were obtained by analyzing populations of bubbles $\geq$ 20μm diameter; the read out time will be further increased if smaller bubbles are included in the analysis. Automatic evaluation of holographically recorded particle populations will probably solve these problems. However this technique is still in its infancy. The reader is referred to the very interesting work of Bexon et al. [4, 7] and of Heidt et al. [8] on this matter.

3. DEPTH AND RESOLUTION OF FAR-FIELD RECONSTRUCTIONS

The total optical pathlength Z between the particle and the recording medium is given by $Z=z_1/n_1+z_2/n_2+z_3/n_3$, where $z_{1,2,3}$ and $n_{1,2,3}$ respectively denote the thickness and the refractive index of the media water, glass and air. Fresnel's description of the spatial distribution of the light scattered by a particle of diameter d becomes considerably less complex when the far-field condition $Z>>d^2/\lambda$ is met. In that case quadratic and higher order terms may be neglected and one speaks of Fraunhofer or far-field diffraction [9]. It has been shown [3] that in the far-field region of the individual objects, the reconstruction is not disturbed by background interference with the virtual image. It should be noted however that the recording of particles in the near-field or Fresnel region is by no means prohibited and that excellent reconstructions may be obtained from Fresnel holograms of particles where $Z<<d^2/\lambda$ [6]. Defining the far-field number N as the number of far-field distances d^2/λ between the object and the recording plane, the pathlength becomes $Z=Nd^2/\lambda$ and the far-field number may obviously be formulated in terms of the recording set-up: $N=(\lambda_{ruby}/d^2)(z_1/n_1+z_2/n_2+z_3/n_3)$. On reconstruction of the hologram in air by means of a HeNe-laser the change in wavelength of the illumination and the refractive index of the medium has to be accounted for by $z_i=(\lambda_{HeNe}/\lambda_{ruby})n_i l_i$, where l_i is the reconstructed thickness of the relevant media measured in air. Substitution of this equation in the former renders the far-field number in terms of the reconstructing set-up: $N=\lambda_{HeNe}L/d^2$,

where L is the total distance in air between the reconstructed image and the hologram. As the modulation of the interference fringes is inversely proportional to the far-field number N, at many far-field distances the useful information in the hologram is limited by optical noise such as scattered light, non-uniformity of the reference wave and granularity of the recording medium. Therefore the quality of the reconstructed image in the far-field is limited by a maximum far-field number N_{max} [10]. Different workers have explored the maximum achievable far-field number for acceptable reconstructions. To some degree their results appear to depend on film granularity and practical values are found in the range $30<N_{max}<100$ [6]. The high resolving power of the 8E75HD plates used in the present study (>5000 lines/mm) combined with the uniformity of the single mode beam however appeared to allow reconstructions of particles with far-field numbers exceeding 300, while discrimination between bubbles and solid particles remained possible down to 5μm diameter objects.

4. BOUNDARY LAYER FLOW VISUALIZATION

The two hydrofoils were tested in a wide range of angles of attack α and free-stream velocities V_o. Depending on α and V_o, typical boundary layer flow phenomena were observed such as (1) laminar separation near the nose followed by transition to turbulence without re-attachment (free shear layer), (2) laminar separation near the nose followed by transition to turbulence and re-attachment (short bubble), (3) laminar separation near the nose followed by transition to turbulence and re-attachment further downstream (long bubble), (4) laminar boundary layer with laminar separation downstream followed by transition to turbulence, and (5) laminar boundary layer with normal transition to turbulence. An example of laminar separation followed by transition to turbulence without re-attachment for the NACA 16-012 hydrofoil at $\alpha=12^{o}$ is presented in Fig. 5. Fig. 6 shows transition to turbulence and re-attachment of a long laminar separation bubble for the NACA 4412 hydrofoil at $\alpha=10^{o}$.

5. CAVITATION OBSERVATIONS

The type of cavitation occurring at large angles of attack

is cloud cavitation. The cavities are essentially not attached to the surface. An example is shown in Fig. 7, which is for the NACA 16-012 hydrofoil at $\alpha=12^{\circ}$. In this case the boundary layer flow is characterized by the occurrence of a free shear layer (Fig. 5). At moderate angles of attack sheet cavitation is observed, which is related to the presence of a laminar separation bubble. At small angles of attack and sufficiently high velocities, laminar separation does not occur; in this case bubble cavitation is observed. An example is shown in Fig. 8, which is for the NACA 4412 hydrofoil at $\alpha=2^{\circ}$. A full analysis of these relationships will be presented in [11].

REFERENCES

1. J.H.J. van der Meulen, A holographic study of cavitation on axisymmetric bodies and the influence of polymer additives, Ph.D. Dissertation, Enschede, 1976.
2. J.H.J. van der Meulen, H.J. Raterink, Flow visualization of boundary layers in water by in-line holography, Proc. Int. Symp. on Flow Visualization, Tokyo, 277-282, 1977.
3. J.B. de Velis, G.B. Parrent jr., B.J. Thompson, Image reconstruction with Fraunhofer holograms, J. Opt. Soc. Am. 56, 4, 423-427, 1966.
4. R. Bexon, J. Gibbs, G.D. Bishop, Automatic assessment of aerosol holograms, J. Aerosol Sci. 7, 397-407, 1976.
5. E.M. Gates, J. Bacon, A note on the determination of cavitation nuclei distributions by holography, J. Ship Res. 22, 1, 29-31, 1978.
6. R.L. van Renesse, Report on holographic particle analysis: combined measurements at Delft Hydraulics Laboratory, Report 805.252, Institute of Applied Physics TNO-TH, Delft, 1978.
7. R. Bexon, M.G. Dalzell, M.C. Stainer, In-line holography and the assessment of aerosols, Opt. and Laser Techn., 161-165, August 1976.
8. H. Heidt, R. Furchert, Holographische Tropfengrössenanalyse mit automatischer Auswertung im chemischen Pflanzenschutz, Microsc. Acta, Suppl. 1, 51-61, 1977.
9. G.B. Parrent jr., B.J. Thompson, On the Fraunhofer (far-field) diffraction patterns of opaque and transparent objects with coherent background, Optica Acta 11, 3, 182-193, 1964.

10. J.B. de Velis, G.O. Reynolds, Theory and Applications of Holography, Addison-Wesley, Reading Mass., 1967.
11. J.H.J. van der Meulen, Boundary layer and cavitation studies of NACA 16-012 and NACA 4412 hydrofoils, Proc. 13th Symp. on Naval Hydr., Tokyo, October 1980.

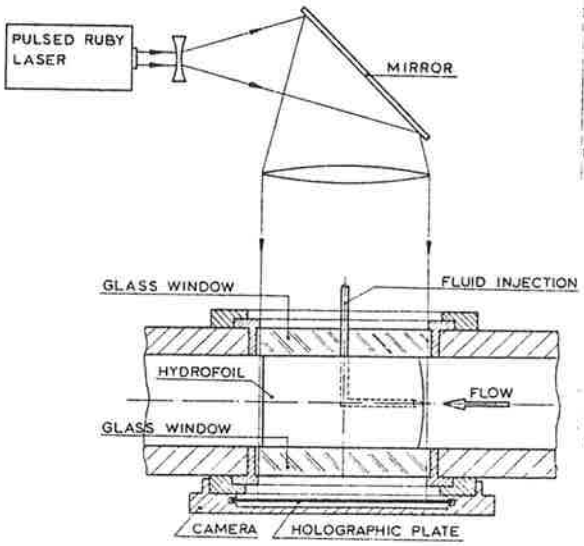

Fig. 1 Schematic diagram of in-line holographic system for making holograms of cavitation and flow phenomena on hydrofoils.

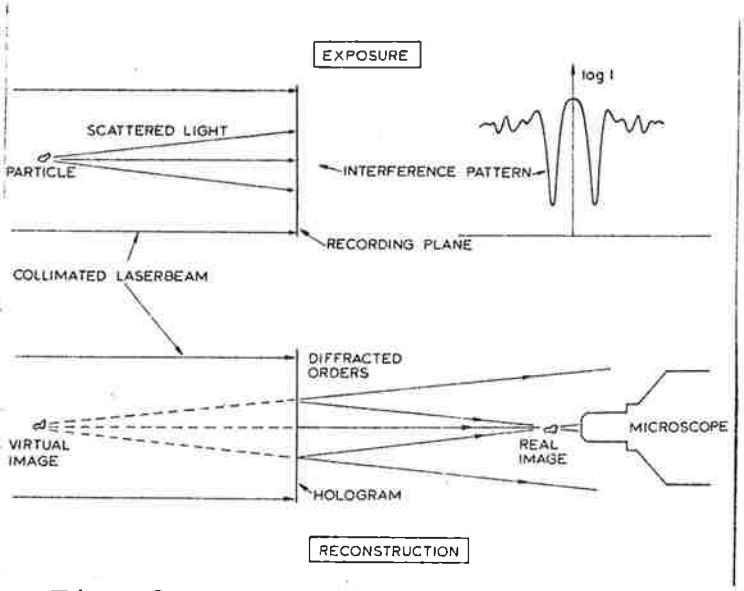

Fig. 2 Schematic view of exposure and subsequent reconstruction of holographed test volume.

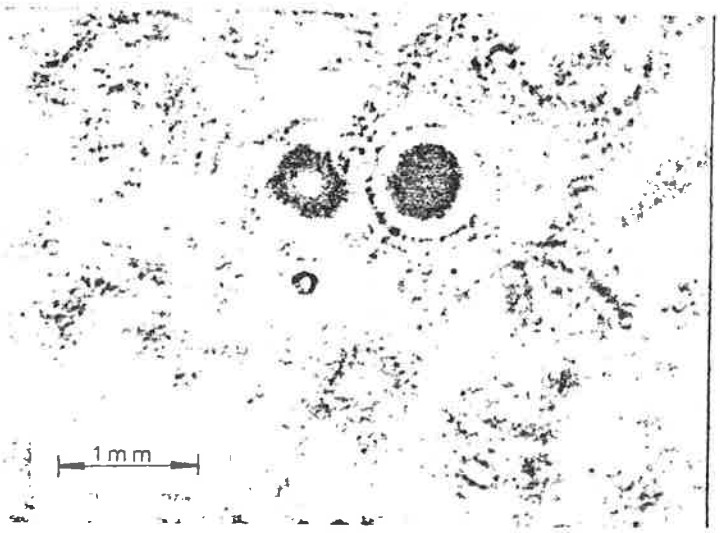

Fig. 3 Typical example of bubble-fringes in the recording plane.

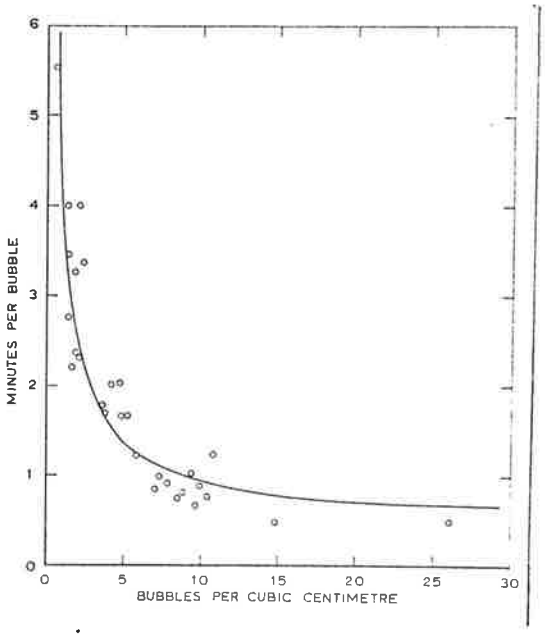

Fig. 4 Data collection time versus bubble concentration for a series of 30 holograms of a test volume in a water tunnel [6].

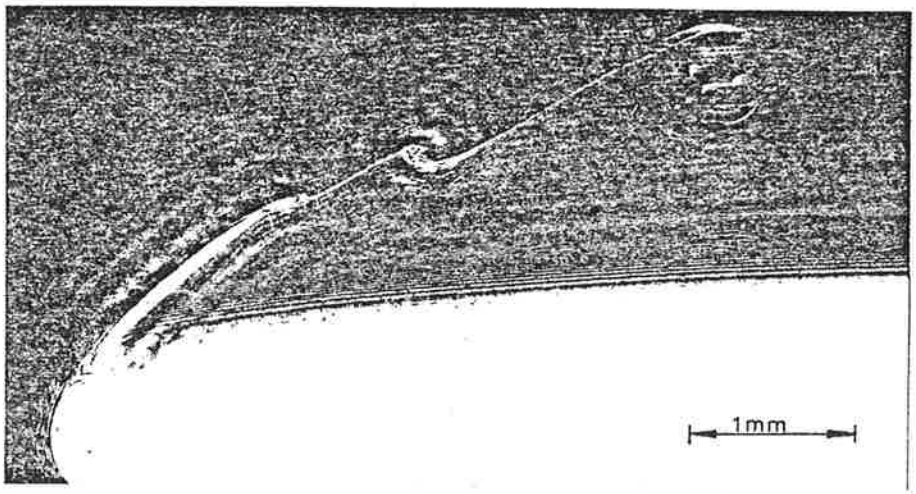

Fig. 5 Separated shear layer for NACA 16-012 hydrofoil at $\alpha=12^{o}$. The flow is from left to right. $V_o=0.9$ m/s.

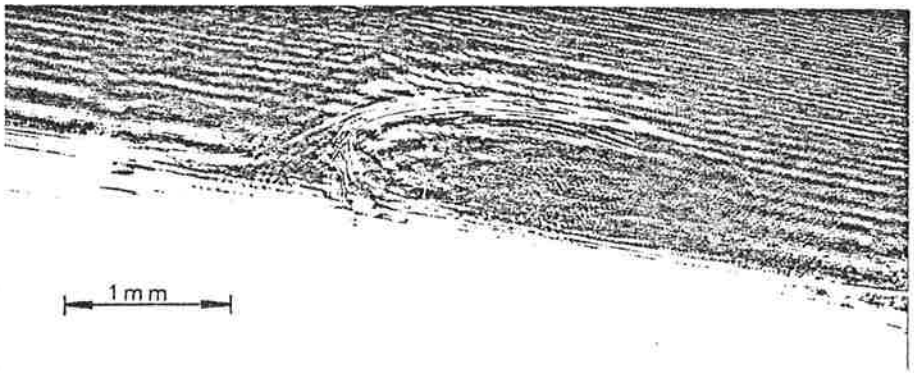

Fig. 6 Transition to turbulence and reattachment of long separation bubble for NACA 4412 hydrofoil at $\alpha=10^{o}$. The flow is from left to right. $V_o=0.9$ m/s; $x_T/c=0.40$.

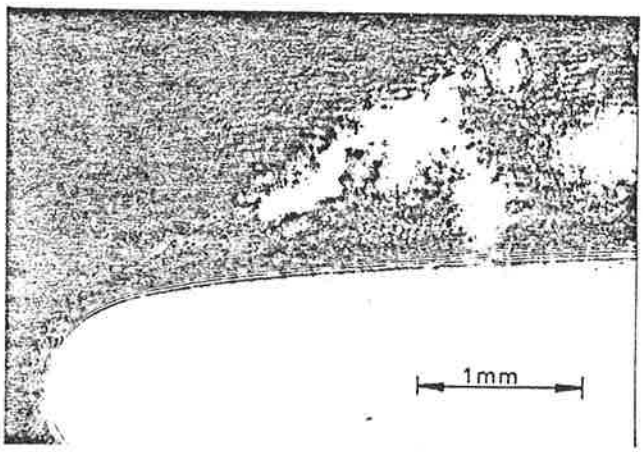

Fig. 7 Cloud cavitation for NACA 16-012 hydrofoil at $\alpha=12^{o}$. The flow is from left to right. $V_o=7.0$ m/s; $\sigma=3.21$.

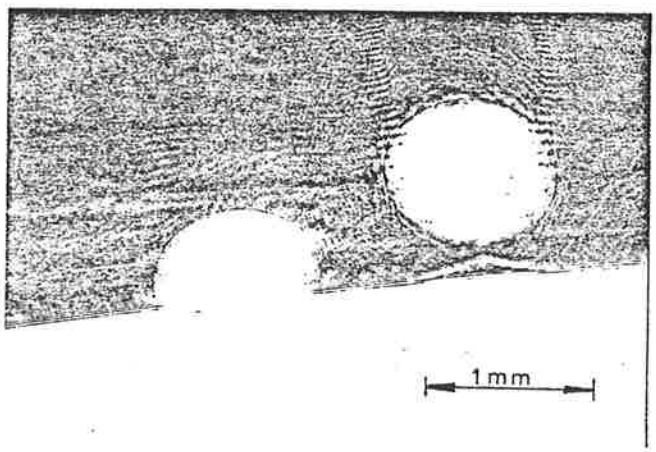

Fig. 8 Bubble cavitation for NACA 4412 hydrofoil at $\alpha=2^{o}$. The flow is from left to right. $V_o=14.9$ m/s; $\sigma=0.85$; $x_c/c=0.17$.